Supporting Information

Improved Solid Electrolyte Conductivity via Macromolecular Self-Assembly: From Linear to Star Comb-like P(S-*co*-BzMA)-*b*-POEGA Block Copolymer

Kingsley Ikenna Aniagbaoso,[1] Monika Król,[2] Janne Ruokolainen,[2] Antoine Bousquet,[1] Maud Save,[1] Laurent Rubatat[1*]

[1] *Universite de Pau et des Pays de l'Adour, E2S UPPA, CNRS, IPREM, Pau, France*

[2] *Department of Applied Physics, School of Science, Aalto University, Espoo FIN-00076, Finland*

* Corresponding author: laurent.rubatat@univ-pau.fr

Individual conversions of monomers (x_{BzMA} and x_S) were calculated from ^{1}H NMR spectra using the aromatic group (copolymer and monomers) in BzMA and S as internal standard, Eq. S1 and Eq S2 respectively.

$$x_{BzMA} = \frac{\left[I_{1H,BzMA(5.6ppm)}\right]_t / \left[I_{1H,\ IS\ (7.5-6.4ppm)} - I_{1H,\ S(5.8ppm)}\right]_t}{\left[I_{1H,BzMA(5.6ppm)}\right]_0 / \left[I_{1H,\ IS\ (7.5-6.4ppm)} - I_{1H,\ S(5.8ppm)}\right]_0} \quad \text{S1}$$

$$x_S = \frac{\left[I_{1H,S(5.8ppm)}\right]_t / \left[I_{1H,\ IS\ (7.5-6.4ppm)} - I_{1H,\ S(5.8ppm)}\right]_t}{\left[I_{1H,BzMA(5.6ppm)}\right]_0 / \left[I_{1H,\ IS\ (7.5-6.4ppm)} - I_{1H,\ S(5.8ppm)}\right]_0} \quad \text{S2}$$

$I_{1H,BzMA(5.6ppm)}$ corresponds to the integral of one vinyl proton of BzMA at 5.6 ppm, $I_{1H,\ IS\ (7.5-6.4ppm)}$ corresponds to the integral of all 5 polymeric protons and 6 monomeric protons of the aromatic groups of BzMA and S plus 1 vinyl proton of S, $I_{1H,\ S(5.8ppm)}$ corresponds to the integral of one vinyl proton of S (5.8 ppm, 1H). it is important to say that the NMR of the kinetics were performed in $CDCl_3$ (7.25 ppm) and contributes ≈ 5 % error to the calculation.

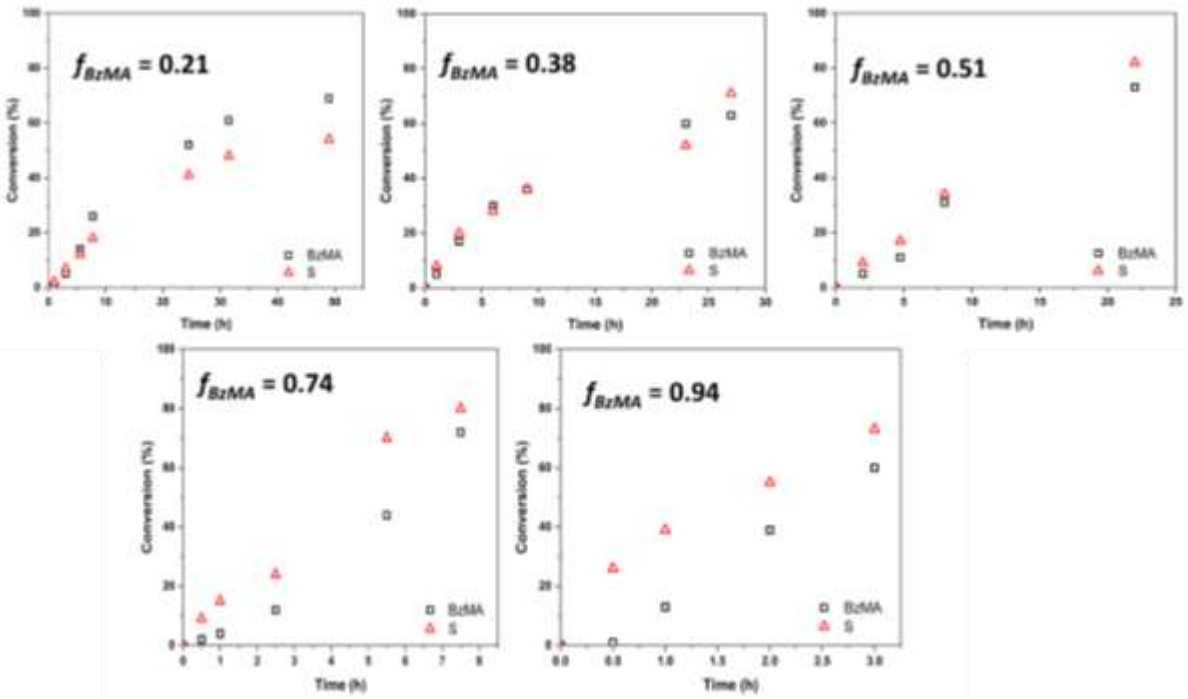

Figure S1. Individual molar conversion of benzyl methacrylate and styrene over time during RAFT polymerization.

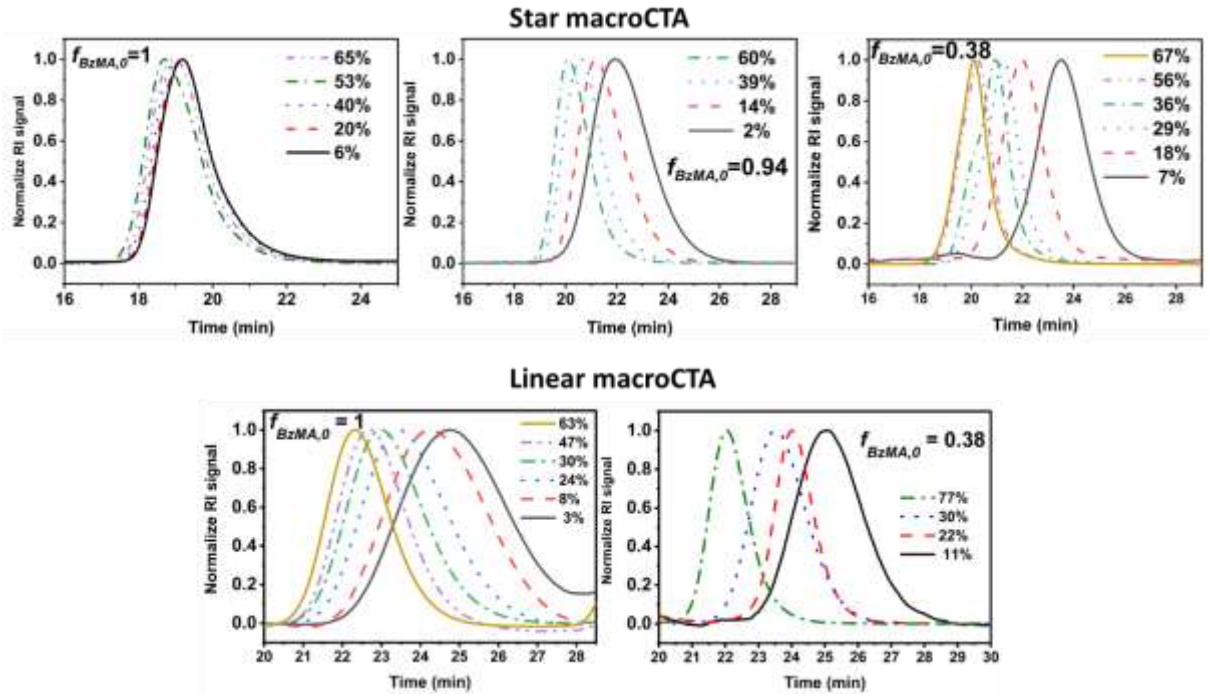

Figure S2. Evolution of the size exclusion chromatogram (RI trace) with monomer conversion for star (up) and linear (down) copolymers at different feed ratios.

The final overall molar and weight conversions (X_m and X_w respectively) were calculated from the individual monomer conversions according to Eq S3 and Eq. S4 (n_0 and m_0 respectively corresponds to the initial number of moles and the initial mass of each monomer).

$$X_m = \frac{(x_{BzMA} \times n_{0,BzMA}) + (x_S \times n_{0,S})}{(n_{0,BzMA} + n_{0,S})} \quad \text{S3}$$

$$X_w = \frac{(x_{BzMA} \times m_{0,BzMA}) + (x_S \times m_{0,S})}{(m_{0,BzMA} + m_{0,S})} \quad \text{S4}$$

The initial molar fraction corresponds to the initial number of moles from the mass of each monomer (see Eq S5).

$$f_{BzMA,0} = \frac{(m_{0,BzMA}/M_{BzMA})}{(m_{0,BzMA}/M_{BzMA}) + (m_{0,S}/M_S)} \quad \text{S5}$$

The experimental fraction of BzMA (f_{BzMA}) in the monomer feed at time, t was calculated from Eq S6.

$$f_{BzMA} = \frac{I_{1H,BzMA(5.6ppm)}}{\left(I_{1H,S(5.8ppm)} + I_{1H,BzMA(5.6ppm)}\right)} \quad \text{S6}$$

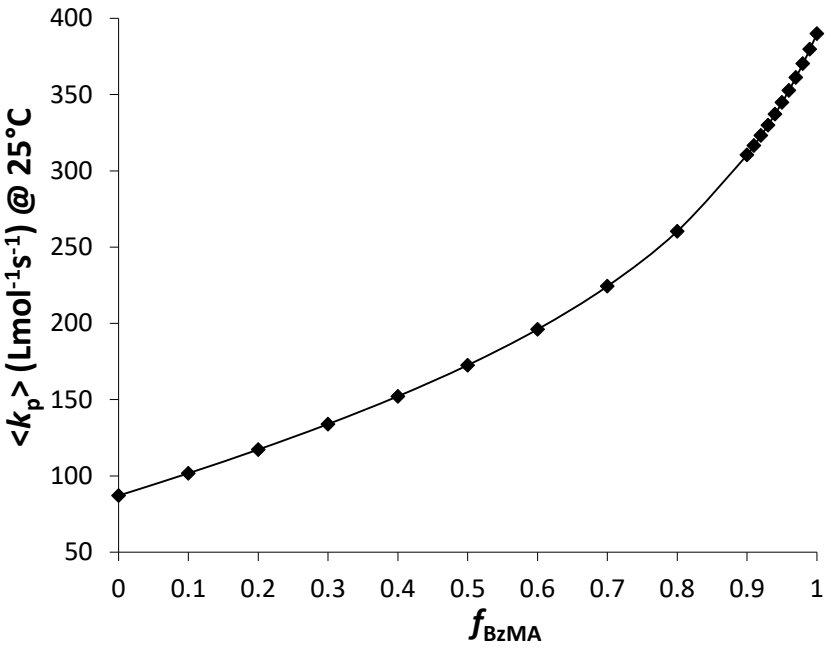

Figure S3. Estimation of the average rate constant of copolymerization (<k_p >) at 25°C for styrene and benzyl methacrylate radical copolymerization based on Eq S7.

$$< k_p > = \frac{r_{BzMA} f_{BzMA}^2 + 2 f_{BzMA} f_S + r_S f_S^2}{r_{BzMA} \frac{f_{BzMA}}{k_{p,BzMA}} + r_S \frac{f_S}{k_{p,S}}} \qquad \text{S7}$$

In Figure 3 and Figure S4, the theoretical values of f_{BzMA} are calculated step-by-step from Eq S8.

$$f_{BzMA,x} = \frac{f_{BzMA,x-dx} - F_{BzMA,\ theo} \cdot dx}{\left(f_{BzMA,x-dx} - F_{BzMA,\ theo} \cdot dx\right) + \left(f_{S,x-dx} - F_S \cdot dx\right)} \qquad \text{S8}$$

With x the monomer conversion and dx as the change in monomer conversion (dx set at 0.1) and by using Lewis-Mayo equation (Eq S9) for determination of $F_{BzMA,\ theo}$.

$$F_{BzMA,\ theo.} = \frac{r_{BzMA} \times f_{BzMA}{}^2 + f_{BzMA} \times f_S}{r_{BzMA} \times f_{BzMa}{}^2 + 2 \times f_{BzMA} \times f_S + r_S \times f_S{}^2} \qquad \text{S9}$$

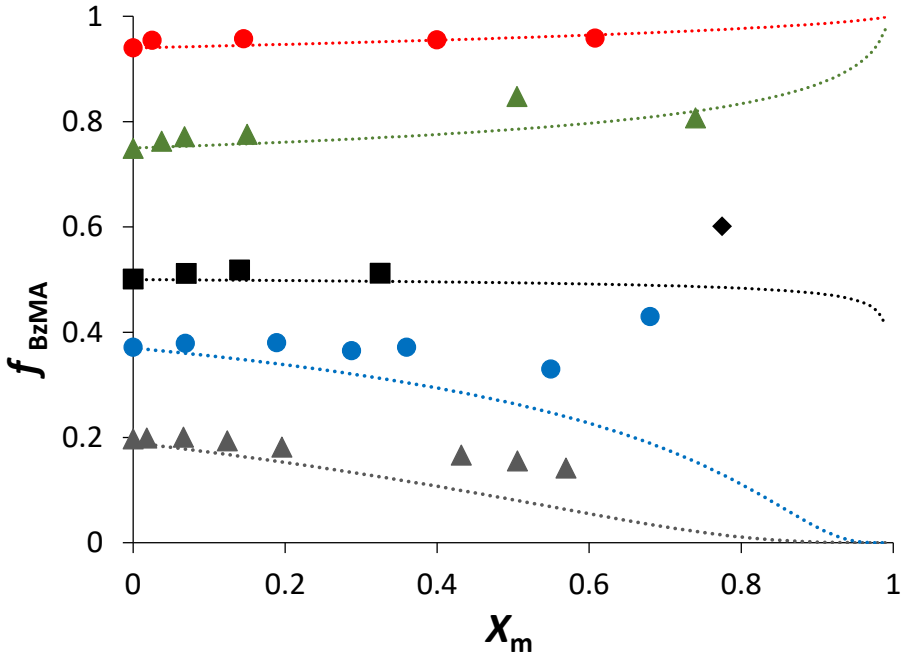

Figure S4. Evolution of BzMA fraction in monomer feed with X_m conversion. ▲ $f_{BzMA,0}$ = 0.19, ■ $f_{BzMA,0}$ = 0.38, ◆ $f_{BzMA,0}$ = 0.50, ▲ $f_{BzMA,0}$ = 0.75, ● $f_{BzMA,0}$ = 0.94. The dotted line corresponds to the fit of f_{BzMA} versus conversion calculated from Eq S8 by using reactivity ratios of reference [1] (r_S = 0.27 ± 0.14, r_{BzMA} = 0.86 ± 0.36).

The molar fraction of the BzMA monomer incorporated into the copolymer ($F_{BzMA,\beta}$) was calculated from the individual monomer conversions (x_{BzMA} and x_S) and the initial number of moles of monomer ($n_{0,BzMA}$ and $n_{0,S}$), according to Eq S10.

$$F_{BzMA,\beta} = \frac{x_{BzMA} \times n_{0,BzMA}}{x_{BzMA} \times n_{0,BzMA} + x_S \times n_{0,S}} \qquad \text{S10}$$

The molar fraction of BzMA in the copolymer after purification ($F_{BzMA,\alpha}$ and $F_{BzMA,\gamma}$)) was calculated from ^{1}H NMR in $CDCl_3$ and CD_2Cl_2 respectively is given by Eq S11. The integral of the peak from 5 ppm to 3 ppm corresponds to 2 protons of PBzMA in the copolymer and the integral of the peak from 7.5 ppm to 6.4 ppm corresponds to the 5 protons of benzyl group of PBzMA and PS. $CDCl_3$ constitutes an error of ± 5% owing to the presence of hydrogen peak at 7.26 ppm.

$$F_{BzMA,\gamma} = \frac{I_{1H,PBzMA}\ units}{\left[I_{1H,PBzMA}\ units\ + I_{1H,PS}\ units\right]} \qquad \text{S11}$$

The weight fraction of BzMA in the copolymer (W_{BzMA}) was obtained from Eq S12, considering the molar fraction of the BzMA monomer ($F_{BzMA,\gamma}$) in the purified copolymer measured in

CD_2Cl_2 and the molar masses of each monomer ($M_{BzMA} = 176\ g.mol^{-1}\ and\ M_S = 104\ g.mol^{-1}$).

$$W_{BzMA,\gamma} = \frac{\left(F_{BzMA,\gamma} \times M_{BzMA}\right)}{\left(F_{BzMA,\gamma} \times M_{BzMA}\right) + \left((1 - F_{BzMA,\gamma}) \times M_S\right)} \quad \text{S12}$$

The values of refractive index increment (dn/dc) of the copolymers in THF was calculated using Eq S13 as found in literature.[2] $dn/dc_{\mathrm{PBzMA}} = 0.151$ mL g^{-1}, $dn/dc_{\mathrm{PS}} = 0.185$ mL g^{-1}, and $dn/dc_{\mathrm{POEGA}} = 0.062$ mL g^{-1}were respectively taken from references. [3-5] The *dn/dc* describes how much the refractive index of a copolymer solution changes with respect to the concentration of the solute. Calculated values of dn/dc of P(S-co-BzMA) macroCTA and P(S-co-BzMA)-b-POEGA block copolymer were are reported respectively in

Table S1 and

Table S*2* determined by Eq S13. These values are expected to match experimental ones according to literature.[2]

$$\frac{dn}{dc}_{macroCTA} = W_{BzMA,\gamma}\left(\frac{dn}{dc}\right)_{PBzMA} + W_{S,\gamma}\left(\frac{dn}{dc}\right)_{PS}$$

$$\frac{dn}{dc}_{BC} = W_{macroCTA,\gamma}\left(\frac{dn}{dc}\right)_{macroCTA} + W_{POEGA,\gamma}\left(\frac{dn}{dc}\right)_{POEGA} \quad \text{S13}$$

The experimentally determined molar mass ($M_{n,MALLS}$) were compared to the theoretical number-average molar mass ($M_{n,theo}$) of the macroCTA and BC calculated from Eq S14 and S15 respectively.

$$M_{n,theo}\ macroCTA = M_{TTC} + X_w \frac{(m_{0,S} + m_{0,BzMA})}{n_{0,TTC}} \quad \text{S14}$$

$$M_{n,theo}\ \text{BCP} = M_{n,MALLS,macroCTA} + \frac{x_{PEGA} \times [OEGA]_0}{[\text{macroCTA}]_0} \quad \text{S15}$$

Table S1: Summary of Initial Monomer Feed Composition, Final BzMA fraction in the copolymer calculated from different methods, values of refractive index increment and Macromolecular Features of the P(S-*co*-BzMA) macro-CTA Synthesized by RAFT copolymerization in bulk

Macro-CTA	$f_{BzMA,0}$ [1]	X_m [2]	X_w [3]	$F_{BzMA,\beta}$ [4]	$F_{BzMA,\alpha}$ [5]	$F_{BzMA,\gamma}$ [6]	$\frac{dn}{dc}_{Poly}$ [7] (mL g^{-1})	$M_{n,MALLS}$ [8] (kg·mol^{-1})
***l*-A$_{1.0}$**	1	-	62	1	1	1	0.151	38
***l*-A$_{0.59}$**	0.38	-	76	0.39	0.43	0.46	0.169	28
***l*-A$_{0}$**	0	-	52	0	0	0	0.185	22
***s*-A$_{1.0}$**	1	65	65	1	1	1	0.151	217
***s*-A$_{0.98}$**	0.92	60	60	0.93	0.96	0.97	0.152	123
***s*-A$_{0.86}$**	0.74	74	73	0.73	0.75	0.78	0.155	152
***s*-A$_{0.71}$**	0.51	77	76	0.47	0.50	0.58	0.160	134
***s*-A$_{0.62}$**	0.38	69	68	0.36	0.44	0.49	0.163	122
***s*-A$_{0.43}$**	0.21	59	57	0.24	0.30	0.31	0.170	80
***s*-A$_{0}$**	0	52	52	0	0	0	0.185	122

[1] BzMA molar fraction in the initial feed.
[2] Overall molar conversion of monomers, Eq S3.
[3] Overall weight conversion of monomers, Eq S4.
[4] $F_{BzMA,\beta}$ is the molar fraction of the monomer into the copolymer calculated from individual monomer conversion determined by NMR-$CDCl_3$, Eq S10.
[5] Molar fraction of the monomer into the copolymer after purification determined by NMR-$CDCl_3$, Eq S11.
[6] Mole fraction of the monomer in the copolymer after purification by NMR-CD_2Cl_2, Eq S11.
[7] Refractive index increments of the copolymer determined from Eq S13.
[8] M_n values obtained from the SEC analysis with a MALLS detector.

The Extended Kelen-Tüdös (e-KT) method: The copolymer composition (F_{BzMA}) of the purified polymer was determined in CD_2Cl_2. The reactivity ratios are estimated through linear regression of the experimental data fitted by the relationship of equation S16.

$$\eta = \left[r_{BzMA} + \left(\frac{r_S}{\alpha}\right)\right] \times \zeta - \frac{r_S}{\alpha} \qquad \text{S16}$$

Where $= \frac{G}{(\alpha+F)}$, $\zeta = \frac{F}{(\alpha+F)}$, with $\alpha = (F_{min} \times F_{max})^{1/2}$,

$G = \frac{\left(F_{BzMA}/F_S\right)-1}{z}$ and $F = \frac{\left(F_{BzMA}/F_S\right)}{z^2}$ where $z = \frac{ln(1-x_{BzMA})}{ln(1-x_S)}$

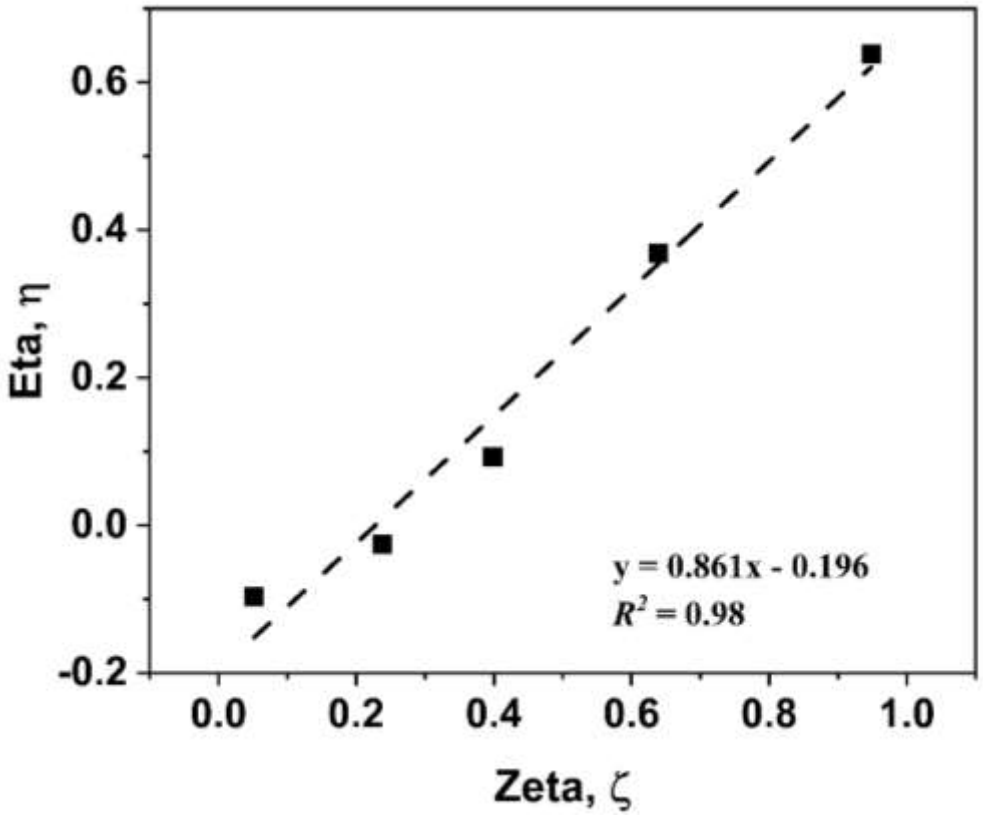

Figure S5. Plot of Eta, η vs Zeta, ζ from Eq S16.

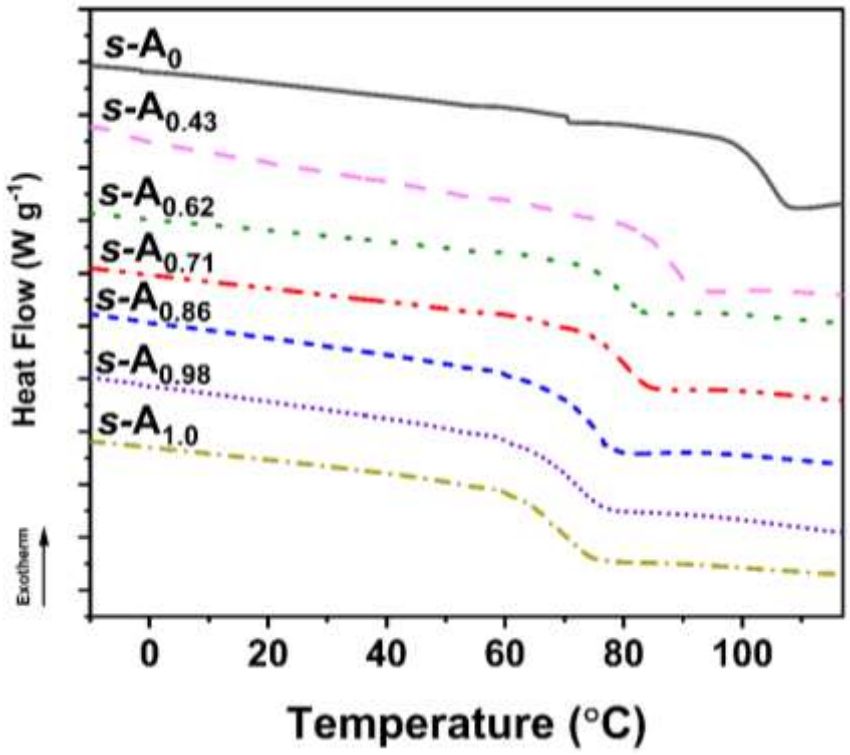

Figure S6. Glass transition temperature (T_g) of star P(S-*co*-BzMA) copolymer with increasing content of styrene.

$$\frac{1}{T_{g,theo}} = \frac{W_{BzMA}}{T_{g,BzMA}} + \frac{W_{styrene}}{T_{g,styrene}} \qquad \text{S17}$$

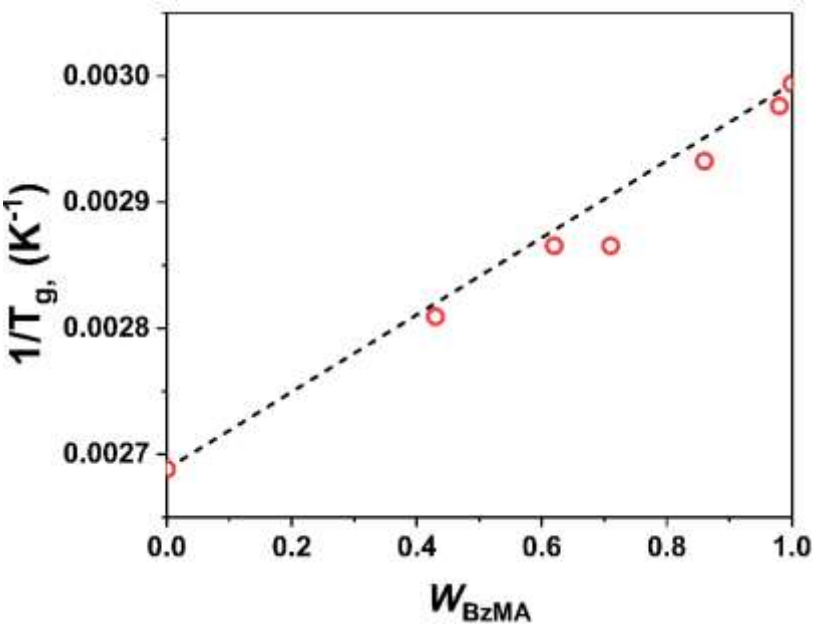

Figure S7. Plot of the weight fraction of BzMA of star macroCTA versus experimental T_g (○). The dotted line corresponds to the theoretical T_g calculated from Eq S17.

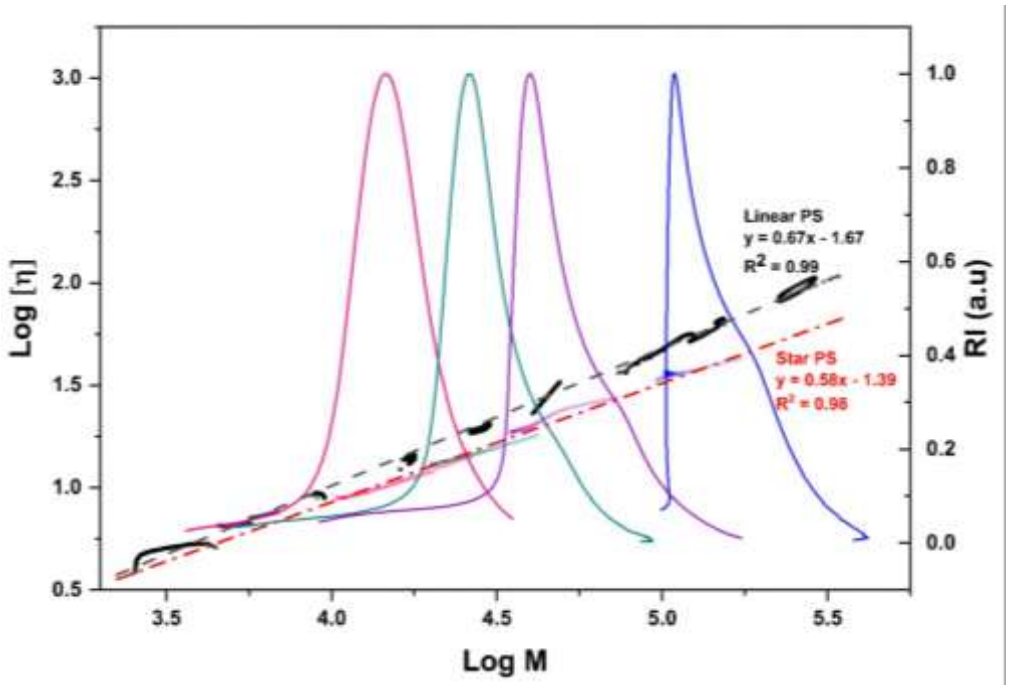

Figure S8. Mark-houwink-sakurada plot for star PS, *s*-A_0, at different monomer conversion with molar mass range 13.7 – 128.7 kg.mol^{-1} (coloured traces/symbols and red linear regression) overlaid with the chromatogram from RI detector to indicate eluting population. Linear PS standards, commercially available for Polystyrene Standard Service PSS supplier (synthesized by anionic polymerization) with molar mass in the range 2.9 – 290 kg.mol^{-1} were used as a basis for comparison (black symbol and black linear regression).

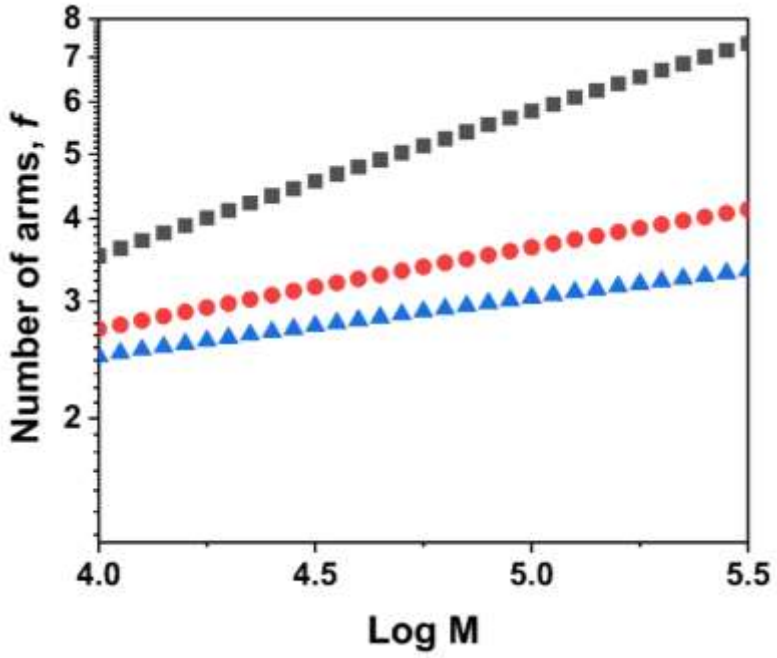

Figure S9. Graph showing the calculated number of arms, *f* versus molar mass (M) of star PS, ***s*-A$_0$**. Shielding ratio ε of 0.5 (■), 1(●) and 1.5 (▲) have been overlaid to show influence of the parameter on the calculated number of arms.

Synthesis of P(S-co-BzMA)-b-POEGA block copolymer by chain extension of macroCTAs.

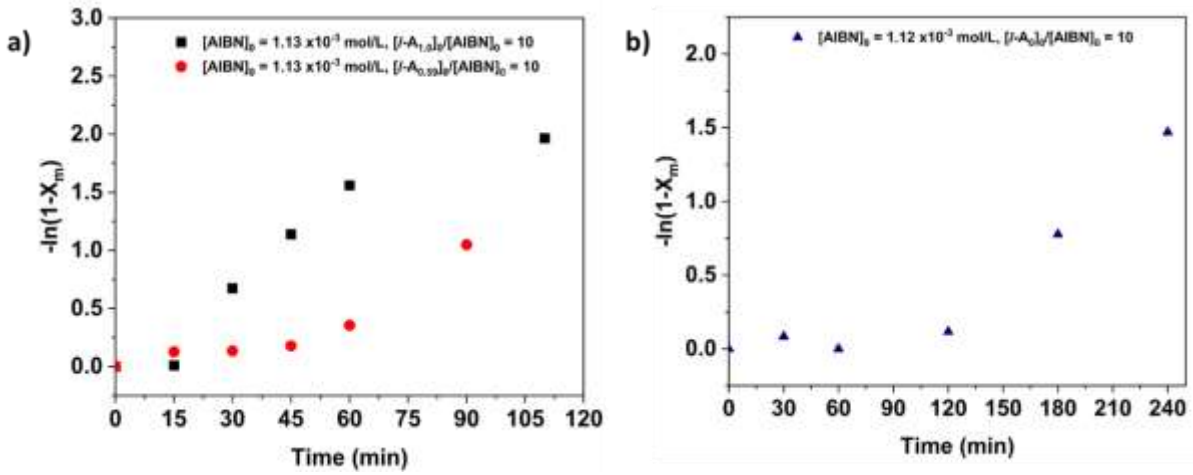

Figure S10. Chain extension of POEGA from linear macro-CTA. (a) PBzMA and P(BzMA-*co*-S) macroCTA in bulk polymerization. (b) PS macro-CTA in solvent polymerization (1,4-dioxane, 1:1 v/v). Polystyrene was in soluble in OEGA monomer, hence solvent polymerization was the only feasible route for block copolymerisation.

The molar conversion of OEGA monomer during block copolymerization (x_{OEGA}) was calculated from ^{1}H NMR in CD_2Cl_2 given by Eq S18, taking the integral of one aromatic proton (7.5 – 6.4 ppm) of P(BzMA-*co*-S) first block as internal standard.

$$x_{OEGA} = 1 - \frac{\left[I_{1H,\,OEGA(5.9ppm)}\right]_t / \left[I_{1H,\,P(S-co-BzMA)}\right]_t}{\left[I_{1H,\,OEGA(5.9ppm)}\right]_0 / \left[I_{1H,\,P(S-co-BzMA)}\right]_0} \qquad \text{S18}$$

The molar fraction of POEGA in the block copolymer after purification (F_{OEGA}) was calculated from ^{1}H NMR in CD_2Cl_2 is given by Eq S19. Where $I_{1H,macroCTA+OEGA}$ is the summation of the integral of 1 aromatic proton of P(S-*co*-BzMA) and 1 proton of POEGA.e and 37 protons of POEGA in the final BCP. $I_{1H,OEGA(5-3ppm)}$is obtained by subtracting peak from 5 ppm to 3 ppm corresponding to 2 protons of PBzMA in the starting macroCTA from BCP and dividing by 37 protons of POEGA.

$$F_{OEGA} = \frac{\left[I_{1H,OEGA(5-3ppm)}\right]}{\left[I_{1H,macroCTA+OEGA}\right]} \qquad \text{S19}$$

The weight fraction of OEGA in the block copolymer (W_{OEGA}) was obtained from Eq S22, considering the molar fraction of the OEGA monomer (F_{OEGA}) in the purified BCP measured in CD_2Cl_2. Where $M_{P(S-co-BzMA)} = (176\ g\ mol^{-1} \times F_{BzMA}) + (104\ g\ mol^{-1} \times F_S)$ and $M_{OEGA} = 480\ g\ mol^{-1}$

$$W_{BzMA,\gamma} = \frac{(F_{OEGA} \times M_{OEGA})}{(F_{OEGA} \times M_{OEGA}) + \left((1 - F_{OEGA}) \times M_{P(S-co-BzMA)}\right)} \qquad \text{S20}$$

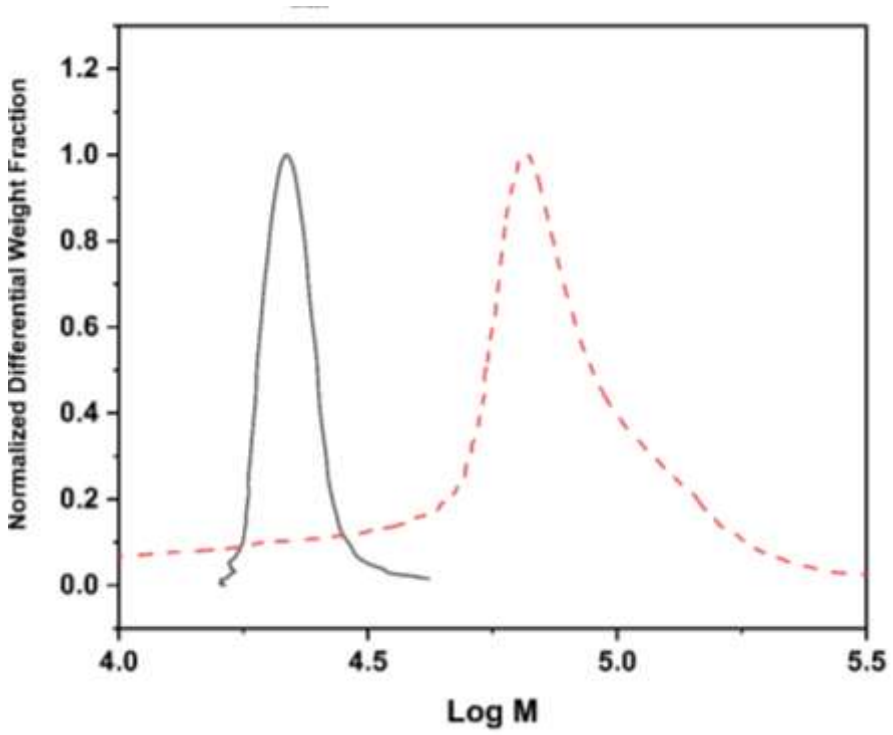

Figure S11. SEC-MALLS traces of *l*-A_0 macroCTA (——) and *lc*-$(A_0)_{0.32}B_{0.68}$ Block copolymer (- - -)

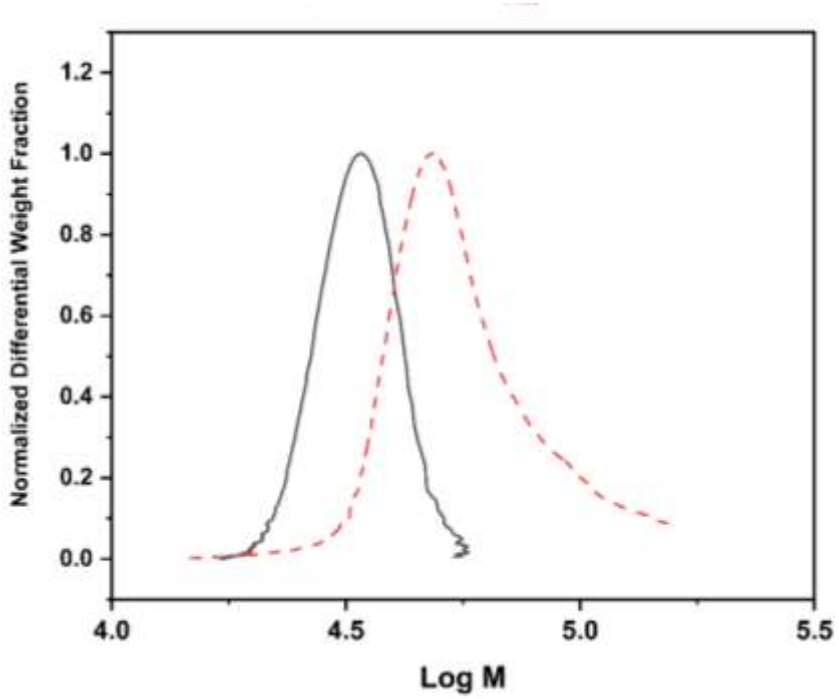

Figure S12. SEC-MALLS analysis of *l*-$A_{0.59}$ macroCTA (──) and *lc*-$(A_{0.59})_{0.71}B_{0.29}$ Block copolymer (- - -).

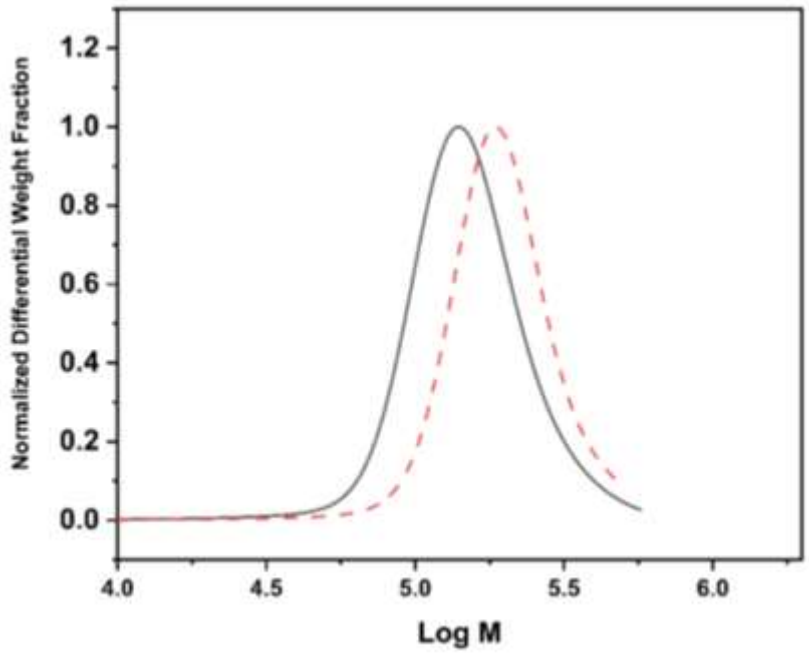

Figure S13. SEC-MALLS analysis of *s*-$A_{0.62}$ macroCTA (──) KA21-A and *sc*-$(A_{0.62})_{0.80}B_{0.20}$ Block copolymer (- - -) KA22-C:

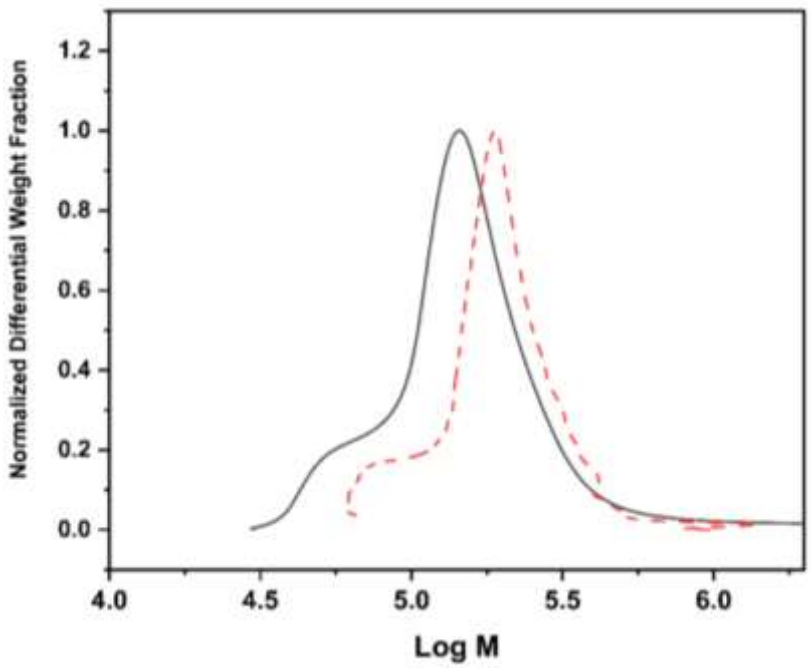

Figure S14. SEC-MALLS analysis of *s*-$A_{0.43}$ macroCTA (—) KA37: and *sc*-$(A_{0.43})_{0.84}B_{0.16}$ Block copolymer (- - -) KA40

Table S2. Features of the AB Linear Comb-like and Star Comb-like Diblock Copolymers Synthesized from the macro-CTA reported in Table 1.

Macro-CTA	W_{POEGA} [a]	dn/dc_{poly} $mL.g^{-1}$	$M_{n,theo}$ [b] (kg·mol^{-1})	$M_{n,SEC\ MALLS}$ (kg·mol^{-1})	$Đ_{SEC\ MALLS}$	BCP[c]
***l*-A_0**	0.68	0.101	59	41	1.20	***lc*-$(A_0)_{0.32}B_{0.68}$**
***l*-$A_{0.59}$**	0.29	0.114	48	41	1.10	***lc*-$(A_{0.59})_{0.71}B_{0.29}$**
***s*-$A_{0.62}$**	0.77	0.085	530	*n.a.* [d]	*n.a.* [d]	***sc*-$(A_{0.62})_{0.23}B_{0.77}$**
***s*-$A_{0.62}$**	0.27	0.138	219	414	1.31	***sc*-$(A_{0.62})_{0.73}B_{0.27}$**
***s*-$A_{0.62}$**	0.20	0.147	153	155	1.22	***sc*-$(A_{0.62})_{0.80}B_{0.20}$**
***s*-$A_{0.43}$**	0.16	0.145	95	109	1.31	***sc*-$(A_{0.43})_{0.84}B_{0.16}$**

[a] W_{POEGA} is the weight fraction of POEGA in the block copolymer after purification, as determined from the molar fraction calculated from ^{1}H NMR spectra (see Eq. S19).
[b] Theoretical molar mass determined from Eq. S14.
[c] *s*- and *l*- represents the star and linear polymers respectively.
[d] The SEC analysis was not applicable as the solubility of samples was too low and refractive index signal at very low intensity to be reliable.

Table S3. Vogel temperature, T_0, determined from VFT fitting together with the corresponding glass transitions, T_g, of the POEGA and LiTFSI phase (B/Li^+ block); both collected on the highest conductive star and linear BCPEs. All BCPEs featured a constant salt concentration [EO]/[Li+] =15. The associated DCS curves are displayed in Figure S15 and VFT fitting in Figure 5.

Polymer	T_0 (°C)[a]	T_g B/Li^+ block (˚C)
***lc*-$(A_0)_{0.32}B_{0.68}$**	-86.3	-40.3
***sc*-$(A_{0.62})_{0.23}B_{0.77}$**	-99.0	-50.8
***sc*-$(A_{0.62})_{0.73}B_{0.27}$**	-91.2	-46.6
***sc*-$(A_{0.62})_{0.80}B_{0.20}$**	-84.0	-22.8

[a]Values of T_0 are determined by fitting conductivity data with VFT model in Eq 3.

Differential Scanning Calorimetry (DSC).

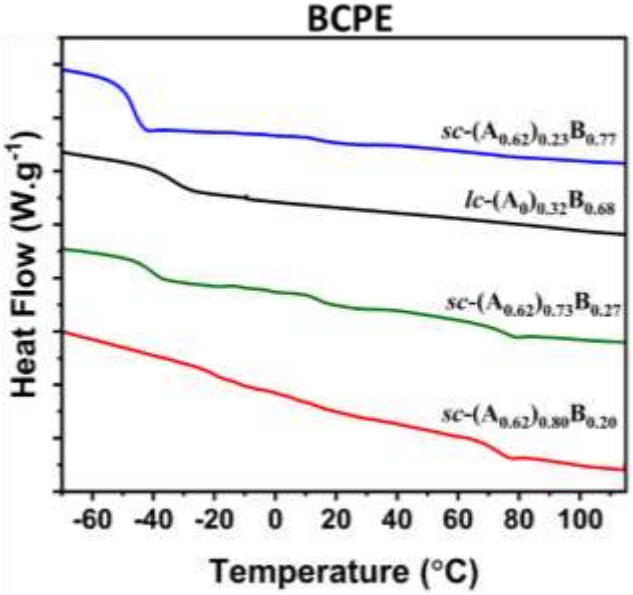

Figure S15. DSC heating curves collected on star and linear BCPEs presented in Table S*3*. The lower Tg values are attributed to the POEGA and LiTFSI phase, and are reported in Table S3.

In Figure S15, the DSC curves of the BCPEs show low T_g values associated to the POEGA and LiTFSI phase increasing from -51 °C to -23 °C with decreasing content of conductive phase. At the lowest conductive phase content, a T_g around 80 °C, associated to the P(S-*co*-BzMA) is observed.

Table S4. Volume fraction of the BCPE conducting phase calculated with Eq S21

Polymer	**[EO]/[Li]**	ϕ_c
***lc*-$(A_0)_{0.32}B_{0.68}$**	15	0.67
***lc*-$(A_{0.59})_{0.71}B_{0.29}$**	15	0.29
***sc*-$(A_{0.62})_{0.23}B_{0.77}$**	15	0.78
***sc*-$(A_{0.62})_{0.73}B_{0.27}$**	15	0.27
***sc*-$(A_{0.62})_{0.80}B_{0.20}$**	15	0.20
***sc*-$(A_{0.43})_{0.84}B_{0.16}$**	15	0.15

The volume fraction of conducting phase of BCPE was calculated from Eq S21.

$$\phi_c = 1 - \left(\frac{M_A/\rho_A}{M_{AB+LiTFSI}/\rho_{AB+LiTFSI}} \right) \quad \text{S21}$$

Where ρ is used to denote density. The density of the copolymer was calculated from Eq S22.

$$\rho_{12} = \rho_1\rho_2(M_1 + M_2)/(\rho_1 M_2 + \rho_2 M_1) \quad \text{S22}$$

Figure S16: Exemplary pictures of self-standing transparent films (ø 16 mm, *L*= 100 µm) derived from block copolymer electrolyte *sc*-$(A_{0.62})_{0.80}B_{0.20}$.

Table S5. Van Krevelen method for estimating density of POEGA[6]

	Number of groups	molar volume ($cm^3\ mol^{-1}$)	Total molar volume ($cm^3\ mol^{-1}$)
-CH2-	9	16.37	**147.33**
(-CH<)	1	10.80	**10.80**
0=C<	1	21.46	**21.46**
-O-	10	10.67	**106.70**
CH3	1	24.58	**24.58**
Total	-	-	**310.87**
OEGA MW ($g\ mol^{-1}$)	480		
Density ($g\ cm^{-3}$)	1.54		

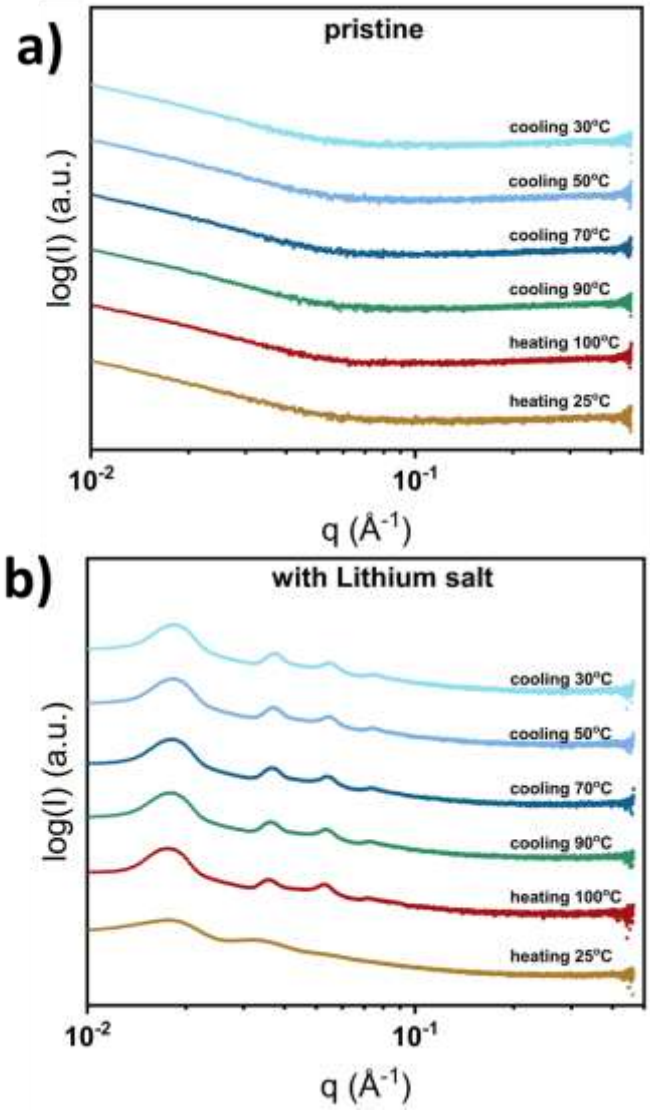

Figure 17. Representative example of SAXS of *in-situ* annealing for *lc*-$(A_{0.59})_{0.71}B_{0.29}$ a) linear BCP b) linear BCPE. Temperature sequence: 25, 100, 90, 70, 50 and 30 °C.

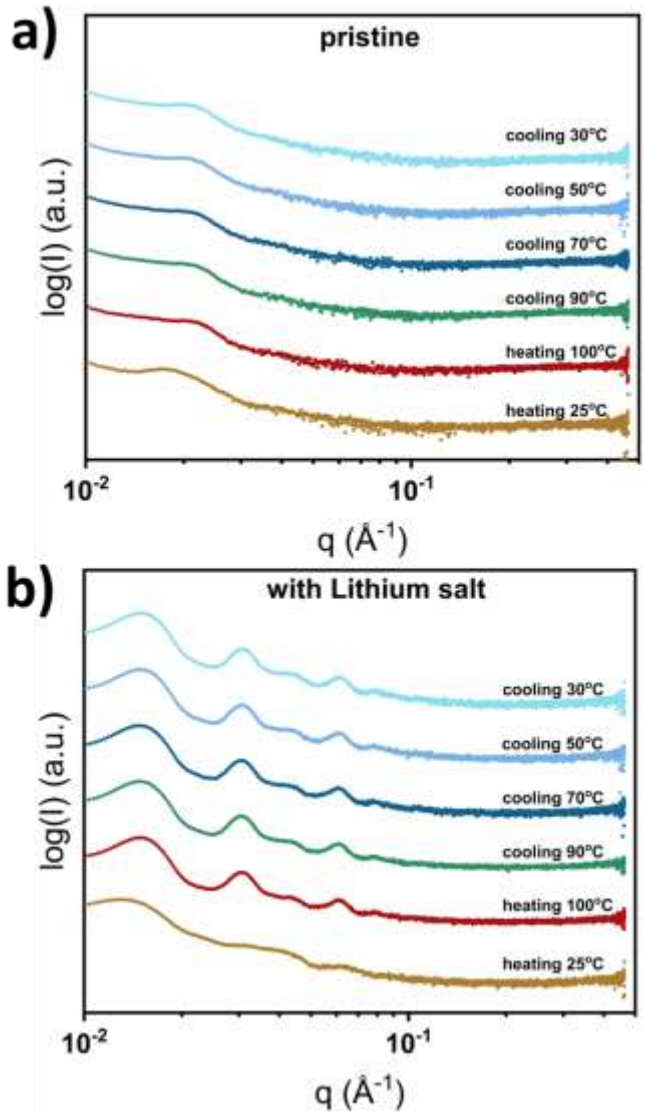

Figure 18. Representative example of SAXS of *in-situ* annealing for *sc*-$(A_{0.62})_{0.80}B_{0.20}$ a) star BCP b) star BCPE. Temperature sequence: 25, 100, 90, 70, 50 and 30 °C.

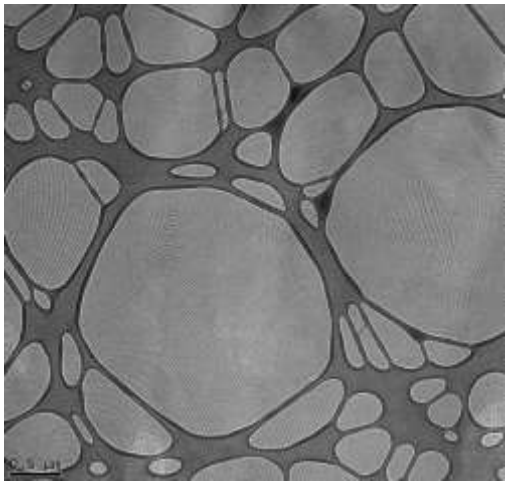

Figure S19. TEM images for annealed star comb-like BCPE: *sc*-$(A_{0.62})_{0.73}B_{0.27}$, $\phi c = 0.27$

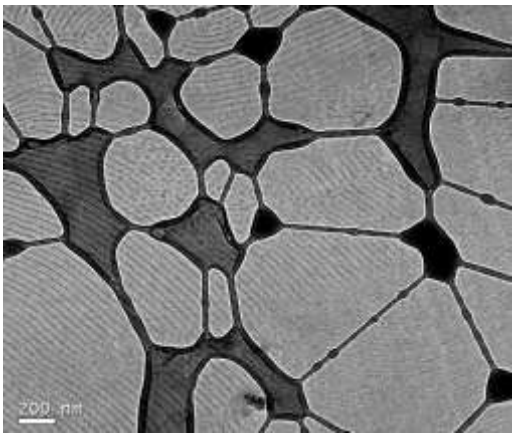

Figure S20. TEM images for annealed star comb-like BCPE: *sc*-$(A_{0.62})_{0.80}B_{0.20}$, ϕc = 0.20

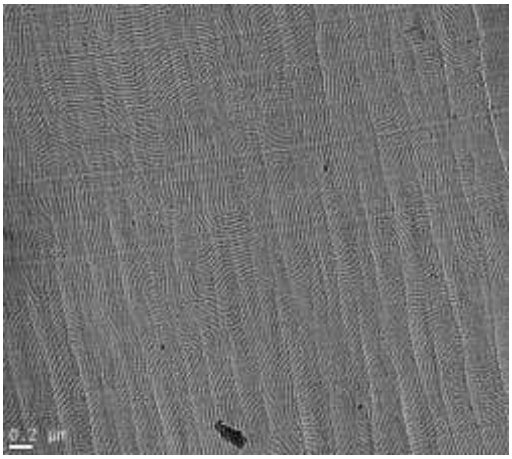

Figure S21. TEM images for annealed linear comb-like BCPE: *lc*-$(A_{0.59})_{0.71}B_{0.29}$, ϕc = 0.29

Table S6. Morphology Factor, *f*, and Tortuosity, τ, for the morphologies of interest[7]

MORPHOLOGY	f	τ
LAM	2/3	1
HEX	1	$(2-\phi_c)$
BCC	1	$(3-\phi_c)/2$

References

(1) Zhang, C.; Lessard, B.; Maric, M. Synthesis and Characterization of Benzyl Methacrylate/Styrene Random Copolymers Prepared by NMP. *Macromolecular Reaction Engineering* **2010,** *4* (6-7), 415-423, DOI: https://doi.org/10.1002/mren.200900069.
(2) Kowalczuk, A.; Mendrek, B.; Żymełka-Miara, I.; Libera, M.; Marcinkowski, A.; Trzebicka, B.; Smet, M.; Dworak, A. Solution behavior of star polymers with oligo(ethylene glycol) methyl ether methacrylate arms. *Polymer* **2012,** *53* (25), 5619-5631, DOI: https://doi.org/10.1016/j.polymer.2012.10.022.

(3) Boissé, S.; Rieger, J.; Belal, K.; Di-Cicco, A.; Beaunier, P.; Li, M.-H.; Charleux, B. Amphiphilic Block Copolymer Nano-Fibers via RAFT-mediated Polymerization in Aqueous Dispersed System. *Chemical Communications* **2010,** *46* (11), 1950-1952, DOI: https://doi.org/10.1039/B923667H.
(4) Aggarwal, R.; Baskaran, D. Synthesis and Dilute Solution Properties of Branched Poly(benzyl methacrylate) Using Na-clay Supported Aqueous-phase Catalysis. *Journal of Polymer Science Part a-Polymer Chemistry* **2018,** *56* (19), 2225-2237, DOI: https://doi.org/10.1002/pola.29193.
(5) Chao, D.; Jia, X.; Tuten, B.; Wang, C.; Berda, E. B. Controlled Folding of a Novel Electroactive Polyolefin via Multiple Sequential Orthogonal Intra-chain Interactions. *Chemical Communications* **2013,** *49* (39), 4178-4180, DOI: https://doi.org/10.1039/C2CC37157J.
(6) Rojas, A. A.; Inceoglu, S.; Mackay, N. G.; Thelen, J. L.; Devaux, D.; Stone, G. M.; Balsara, N. P. Effect of Lithium-Ion Concentration on Morphology and Ion Transport in Single-Ion-Conducting Block Copolymer Electrolytes. *Macromolecules* **2015,** *48* (18), 6589-6595, DOI: https://doi.org/10.1021/acs.macromol.5b01193.
(7) Hallinan, D. T.; Villaluenga, I.; Balsara, N. P. Polymer and Composite Electrolytes. *MRS Bulletin* **2018,** *43* (10), 759-767, DOI: https://doi.org/10.1557/mrs.2018.212.